Article

Ru-Catalyzed Geminal Hydroboration of Silyl Alkynes via a New gem-Addition Mechanism

Qiang Feng, Hao-Nan Wu, Xin Li, Lijuan Song, Lung Wa Chung, Yun-Dong Wu, and Jianwei Sun

J. Am. Chem. Soc., **Just Accepted Manuscript** • DOI: 10.1021/jacs.0c05334 • Publication Date (Web): 15 Jul 2020

Ru-Catalyzed Geminal Hydroboration of Silyl Alkynes via a New *gem*-Addition Mechanism

Qiang Feng,[#] Haonan Wu,[†,‖] Xin Li,[‖] Lijuan Song,[¶] Lung Wa Chung,[‖,*] Yun-Dong Wu,[†,¶,⊥,*] and Jianwei Sun[#,*]

[#] *Department of Chemistry, The Hong Kong University of Science and Technology, Clear Water Bay, Kowloon, Hong Kong SAR, China*

[‖] *Shenzhen Grubbs Institute, Department of Chemistry and Guangdong Provincial Key Laboratory of Catalysis, Southern University of Science and Technology, Shenzhen 518055, China*

[†] *Lab of Computational Chemistry and Drug Design, State Key Laboratory of Chemical Oncogenomics, Peking University Shenzhen Graduate School, Shenzhen 518055, China*

[¶] *Shenzhen Bay Laboratory, Shenzhen 518055, China*

[⊥] *College of Chemistry, Peking University, Beijing 100871, China*

Abstract

While 1,2-addition represents the most common mode of alkyne hydroboration, herein we describe a new 1,1-hydroboration mode. It is the first demonstration of *gem*-(H,B) addition to an alkyne triple bond. With the superior $[CpRu(MeCN)_3]PF_6$ catalyst, a range of silyl alkynes reacted efficiently with HBpin under mild conditions to form various synthetically useful silyl vinyl boronates with complete stereoselectivity and broad functional group compatibility. An extension to germanyl alkynes as well as the hydrosilylation of alkynyl boronates toward the same type products was also achieved. Mechanistically, this process features a new pathway featuring *gem*-(H,B) addition to form the key α-boryl-α-silyl Ru-carbene intermediate followed by silyl migration. It is believed that the orbital interaction between boron and C_β in the coplanar relationship between the boron atom and the ruthenacyclopropene ring preceding boron migration is responsible for the new reactivity. Control experiments and DFT (including molecular dynamics) calculations provided important insights into the mechanism, which excluded the involvement of metal vinylidene intermediate. This study represents a new step forward not only for alkyne hydroboration, but also for other geminal alkyne additions.

Introduction

Vinylboranes are versatile building blocks in organic synthesis, which can serve as not only low-toxic robust nucleophilic partners in a range of C–C bond formation processes with broad functional group compatibility, but also useful precursors toward other versatile building blocks by simple transformations, such as oxidation and reduction.[1] Among the various methods for their synthesis, alkyne hydroboration represents the most straightforward approach.[1c,d] Consequently, this transformation has been a subject of intensive investigations over the past half century.[1-7] Among them, the 1,2-addition mode has been well-established, with the prototype concerted *syn*-addition particularly known as a text-book reaction (Scheme 1).[2] Recently, various elegant catalytic systems have also been developed to achieve *anti*-hydroboration.[3,4] However, in contrast to these 1,2-additions, the 1,1-addition mode (also called *geminal* or *gem*-addition), which adds H–B to the same terminal of the triple bond and requires migration of one alkyne substituent, has been essentially unknown. Notable exceptions are some formal *trans*-hydroborations of *terminal* alkynes that proceed via metal vinylidene or metal acetylide as key intermediates, which require prior substrate rearrangement and thus obviously cannot be applied to internal alkynes.[5,6] Moreover, direct *geminal* H–B addition to a triple bond remains unknown. Herein, we introduce the first example of this type for silyl alkynes via a new *gem*-hydroborated metal-carbene intermediate.

Scheme 1. Introduction to Alkyne Hydroboration

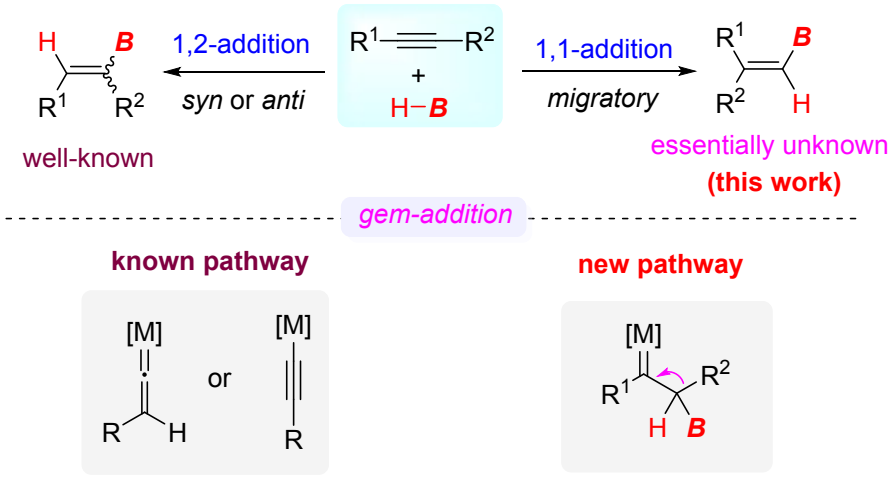

Recently, Fürstner and co-workers have reported a series of pioneering studies on Ru-catalyzed *trans*-1,2-hydrogenation of alkynes, which proceeds via direct *gem*-H_2 addition followed by 1,2-hydrogen migration.[8] However, similar *gem*-(H,B) addition pathway for alkyne hydroboration seemed to be not operative.[3a-c] Instead, the *trans*-1,2-hydroboration was proposed to proceed via a ruthenacyclopropene intermediate, a typical mechanism followed by other related *trans*-hydrometalation processes (e.g., hydrosilylation, hydrostannylation) without involving *gem*-addition.[9] This mechanism is also consistent with the subsequent DFT studies.[3d]

In continuation of our effort in alkyne hydrofunctionalizations,[10] we have recently discovered a *gem*-hydrogenation of silyl alkynes, in which the Fürstner intermediate (*gem*-H_2 carbene) was intercepted by silyl migration.[10b] Inspired by this study and prompted by the important value of alkyne hydroboration, we were curious about the possibility of forming *gem*-(H,B) Ru-carbene with silyl alkynes, which would be

intercepted by silyl migration. This intriguing process would not only lead to synthetically useful silyl vinyl boranes,[11] but more importantly presents a different hydroboration mechanism. However, additional challenges should be expected compared with migratory *gem*-hydrogenation. For example, the *gem*-(H,B)-addition step would experience higher steric repulsion with the silyl group (relative to *gem*-H_2 addition). Secondly, silyl migration would require additional stereocontrol over the resulting olefin configuration to achieve good stereoselectivity.

Results and Discussion

We began our study with silyl alkyne **1a** as the model substrate, in which the phenyldimethylsilyl group ($PhMe_2Si$) was used in view of its general versatility in organic synthesis.[11] The most robust and popular boron reagent, pinacolborane (HBpin), was used as the reaction partner.[2c,d] We first evaluated the [Cp*Ru]-based catalysts in view of their extraordinary performance in alkyne hydrometallation reactions (Table 1, entries 1-4).[3,8-10] Unfortunately, they uniformly exhibited low catalytic activity, and the reaction in DCM proceeded with low conversion at room temperature and gave a mixture of unidentifiable products. It is worth noting that $[Cp^*Ru(MeCN)_3]PF_6$ and $[Cp^*RuCl]_4$ have previously been identified as superior catalysts for 1,2-*trans*-hydroboration of internal alkynes,[3] but unfortunately they resulted in no success in this case. However, to our delight, further screening indicated that $[CpRu(MeCN)_3]PF_6$ showed dramatically high activity (entry 5). More

surprisingly, a silyl-migrated *gem*-hydroboration product **2a** was observed as the sole product in 88% yield. Other Ru-based catalysts, such as those with a strong-coordinating ligand PPh_3 or without the Cp ligand, were completely ineffective (entries 6-7). Remarkably, it is expected that both $PhMe_2Si$ and Bpin in **2a** can be easily and selectively transformed into other useful functional groups. Further optimization of this reaction was performed using other reaction conditions. A higher temperature (50 ^oC) led to slightly lower conversion, presumably due to catalyst decomposition. Increasing the loading of HBpin boosted the reaction efficiency (entry 9). The use of other non-polar halogenated solvents, such as DCE and $CHCl_3$, were almost equally effective as DCM (entries 10-11). However, coordinating solvents like THF, Et_2O and toluene (as π-ligand) essentially shut down the reactivity (entry 12). Notably, replacing the phenyldimethylsilyl group to trimethylsilyl (TMS) in the substrate also failed to give the corresponding product (entry 13). Instead, slow conversion to the regular 1,2-hydroboration products (*Z*/*E* mixture) was observed. Finally, increasing the reaction concentration slightly improved the reaction efficiency (entry 14).

Table 1. Condition Optimization for *gem*-Hydroboration[a]

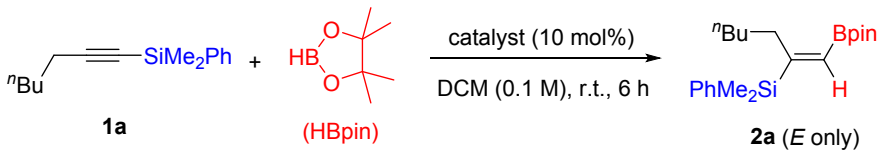

1a (HBpin) **2a** (*E* only)

entry	catalyst or conditions	conversion (%)[b]	yield(%)[b]
1	$[Cp^*Ru(MeCN)_3]PF_6$	13	<5
2	$[Cp^*RuCl]_4$	27	<5
3	$[Cp^*RuCl_2]_n$	29	<5
4	$Cp^*Ru(cod)Cl$	<5	<5
5	$[CpRu(MeCN)_3]PF_6$	94	88
6	$CpRu(PPh_3)_2Cl$	<5	<5
7	$[Ru(cod)Cl]_2$	<5	<5
8[c]	$[CpRu(MeCN)_3]PF_6$	82	72
9[d]	$[CpRu(MeCN)_3]PF_6$	100	92
Deviation from entry 9			
10	DCE as solvent	95	93
11	$CHCl_3$ as solvent	88	83
12	Other coordinating solvents (e.g., Et_2O, THF, MeCN, toluene)	<10	<5
13	TMS in place of $PhMe_2Si$ in **1a**	19	<5
14	*c* = 0.2 M (DCM)	100	94

[a] Reaction scale: **1a** (0.1 mmol), HBpin (0.15 mmol), solvent (1.0 mL). [b] Determined by analysis of the ^1H NMR spectrum of the crude reaction mixture using CH_2Br_2 as an internal standard. [c] Run at 50 °C. [d] Run with 3 equiv of HBpin.

Under the optimized conditions (entry 14, Table 1), a range of substituted silyl alkynes participated in this *gem*-hydroboration process with high efficiency (Table 2). The mild conditions were compatible with a diverse set of functional groups, such as ester, ether, acetal (THP-protected alcohol), silyl ether, mesylate, halide, and phthalimide. Incorporation of heterocycles, such as furan and thiophene, did not affect

the high efficiency. Although the benzene ring was previously known as a good π-ligand for such Ru-systems and can interfere with the catalytic activity,[9g] it was found that the benzyl-substituted alkyne reacted successfully (**2c**). However, direct phenyl-substitution on the alkyne resulted in low conversion. Substitution with a bulky group, such as ^{t}Bu, also led to low reactivity. Notably, in all these successful examples, exclusive *gem*-addition with silyl migration was observed, i.e., no regular 1,2-addition product was detected. Moreover, this addition also features excellent stereoselectivity. The corresponding vinylboronates **2** were all obtained as a single *E*-isomer. The structure of product **2i** was also confirmed by X-ray crystallography.

Table 2. Reaction Scope[a]

1 **2** *single isomer*

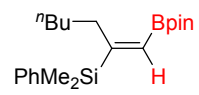

2a, 89%

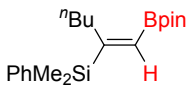

2b, 87%

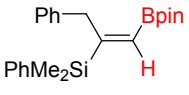

2c, 56%

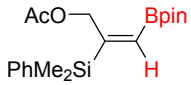

2d, 80%

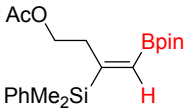

2e, 86%

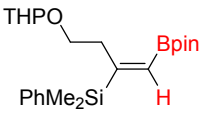

2f, 70%

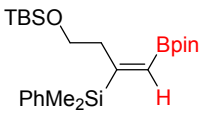

2g, 87%

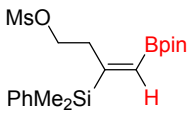

2h, 89%

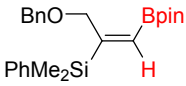

2i, 75%

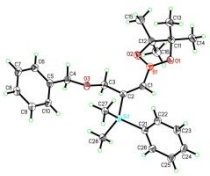

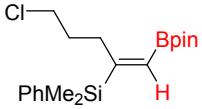

2j, 85%

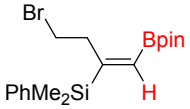

2k, 88%

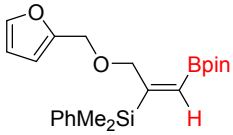

2l, 74%

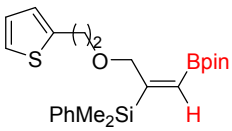

2m, 71%

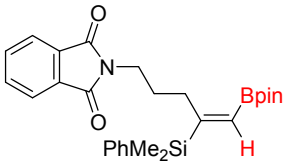

2n, 99%

[a] Reaction scale: **1** (0.3 mmol), HBpin (3 equiv), $[CpRu(MeCN)_3]PF_6$ (10 mol%), DCM (1.5 mL); Isolated yield.

In addition to silyl alkynes, germanyl alkynes also worked well in this *gem*-hydroboration process (eq 1). Under essentially the same conditions, phenyldimethylgermanyl-substituted alkynes **3a** and **3b** reacted efficiently to form the germanyl-migrated vinylboronates **4** with excellent stereoselectivity. The structure was confirmed by X-ray crystallography. It is worth noting that organogermanes are also important building blocks in organic synthesis.[12]

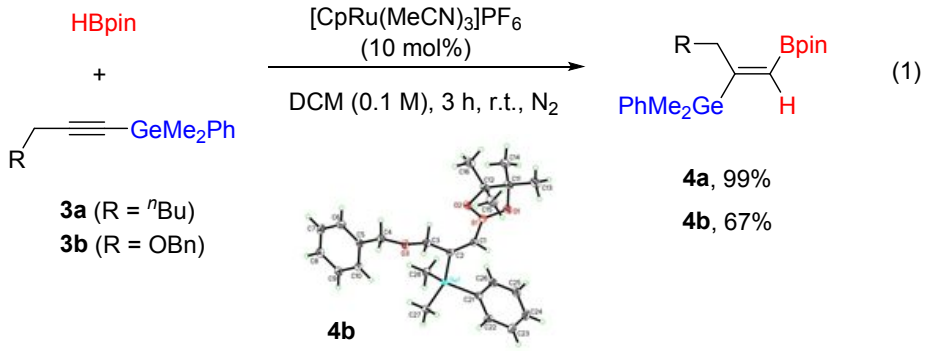

To further investigate the robustness of this *gem*-hydroboration process, we further employed additives with more diverse functional groups to examine their compatibility using the standard reaction of **1a** (Table 3).[13] With aliphatic olefin **5a**, no obvious influence was observed. However, the standard reaction was retarded by aryl olefin **5b**, presumably due to its competing binding with the Ru-catalyst. Regular alkynes **5c-d** had competitive hydroboration reactivity, leading to low conversion of **1a**. The standard reaction was not obviously affected by aldehydes or ketones **5e-g**, although these carbonyl groups could also react with HBpin. It was believed that these carbonyls reacted at a slower rate than **1a**. Moreover, free alcohol **5h**, phenol **5i**, carboxylic acids **5j-k**, azide-tethered phthalimide **5l** and nitrile **5m** also showed good to excellent compatibility with this catalytic system. Unfortunately, the additives with relatively strong-coordinating functionality, such as amide **5n**, thiol **5o**, oxazole **5p**, and thiazole **5q**, significantly retarded this reaction.

Table 3. Study of Functional Group Compatibility[a]

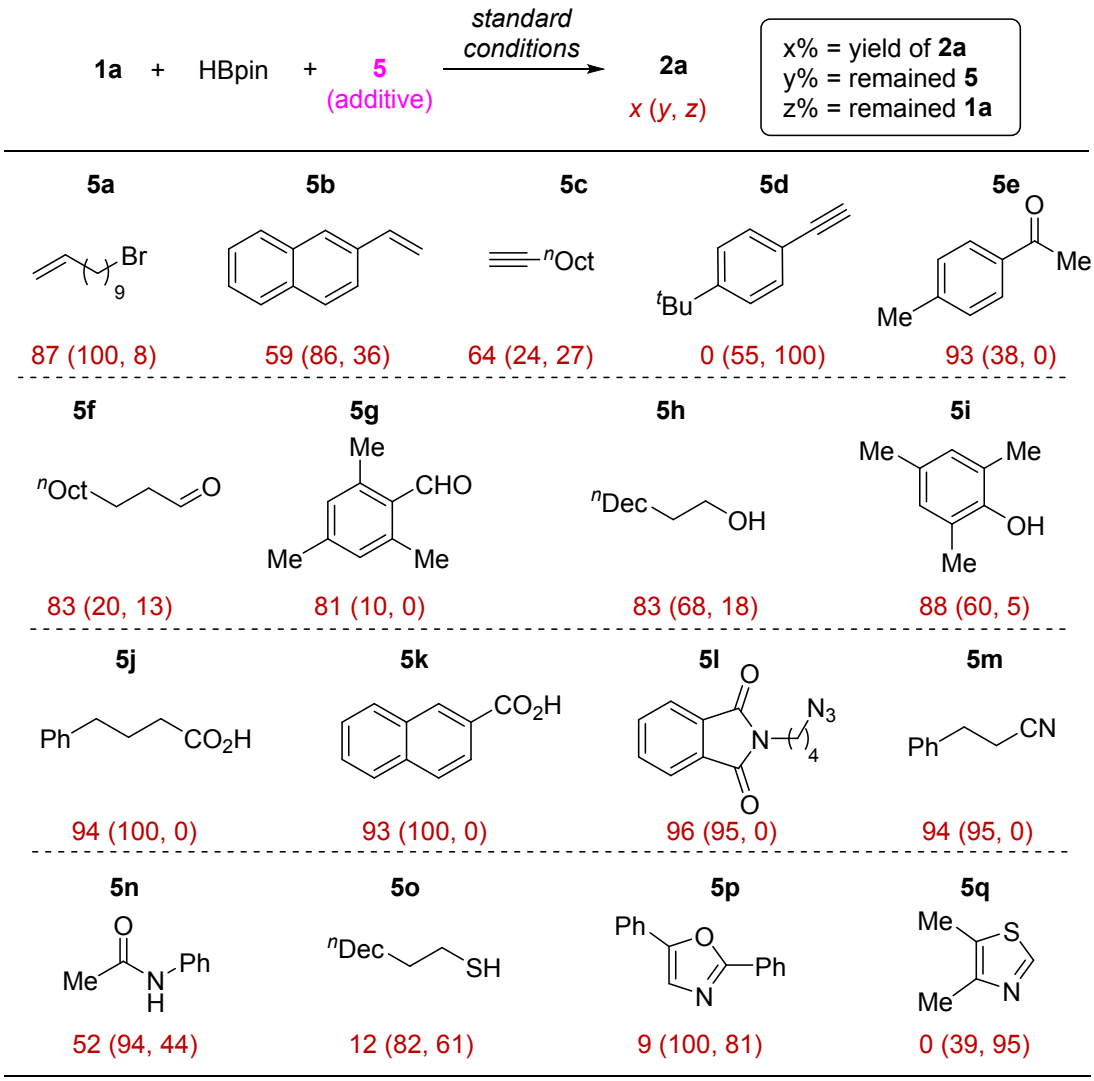

[a] Reaction scale: **1** (0.1 mmol), HBpin (3 equiv), **5** (0.1 mmol), DCM (0.5 mL), r.t., 10 h. Yield was determined by analysis of the ^{1}H NMR spectrum of the crude mixture using CH_2Br_2 as an internal standard.

Next, with the hypothetical mechanism involving *gem*-(H,B) Ru-carbene **IM1** in mind, we further envisioned that this type of α-boryl-α-silyl Ru-carbene might also be generated from *gem*-hydrosilylation of alkynyl boronate substrate **6** (eq 2). In a

similar manner, the subsequent silyl migration should proceed to provide the exactly same type of vinylborane product **2**. If successful, this might lead to not only expanded silyl scope beyond $PhMe_2Si$, but also likely a new hydrosilylation mechanism.

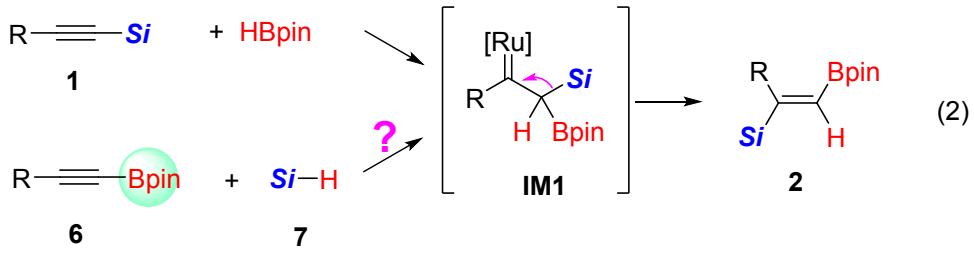

Intrigued by this possibility, we prepared alkynyl boronate **6a** and subjected it to the reaction with $PhMe_2SiH$ under the same conditions (Scheme 2). To our delight, the formal *syn*-hydrosilylation product **2b** was obtained in 85% yield. More importantly, the spectral data indicated that this product was exactly same as that obtained from *gem*-hydroboration. This process exhibited a broad scope with respect to various types of silanes, including Ph_2MeSi, Ph_3SiH, $(EtO)_3SiH$, and Et_3SiH, thereby providing an attractive complement to the above *gem*-hydroboration process. Notably, these products were all obtained as a single isomer as well, highlighting the excellent regio- and stereoselectivity.

Scheme 2. Ru-Catalyzed Hydrosilylation of Alkynyl Boronates[a]

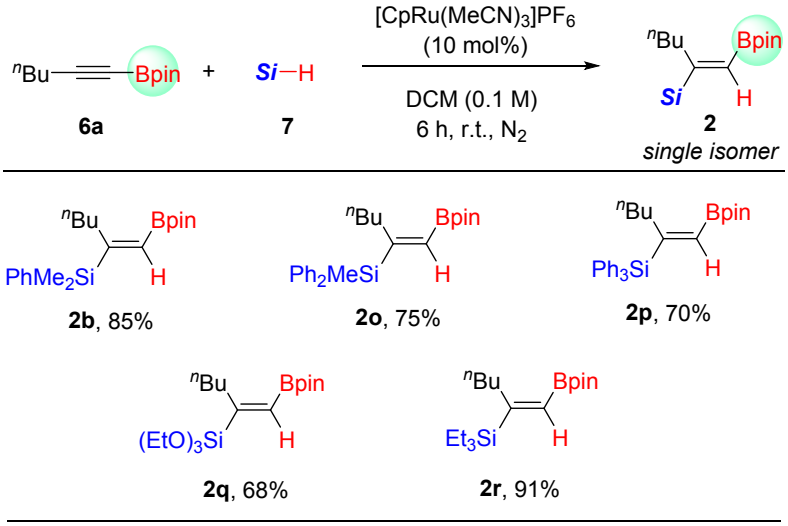

[a] Reaction scale: **6a** (0.3 mmol), **7** (1.5 equiv). Isolated yield.

The products obtained from this reaction can serve as useful precursors to other stereodefined olefins (Scheme 3). The presence of two chemically distinct masking groups (i.e., the silyl and boryl groups) is ideal for sequential transformations with high chemoselectivity. Product **2a** was used to demonstrate these applications. It could serve as a nucleophile for Rh-catalyzed conjugate addition to chalcone, leading to ketone **8** in 84% yield. Moreover, by Cu-catalysis, the boronate motif could selectively react to form vinyl azide **9** and enol ether **10**. With iodine, it could also be converted to vinyl iodide **11**. Furthermore, Pd-catalyzed Suzuki-Miyaura coupling with aryl iodide proceeded selectively to form **12** with excellent efficiency. Finally, the silyl group in **12** could be easily converted to iodide (**13**) upon treatment with NIS,

which would allow further cross-coupling or other transformations when needed. It is worth noting that these transformations not only feature high efficiency and chemoselectivity, but also absolute integrity of the olefin configuration.

Scheme 3. Product Transformations

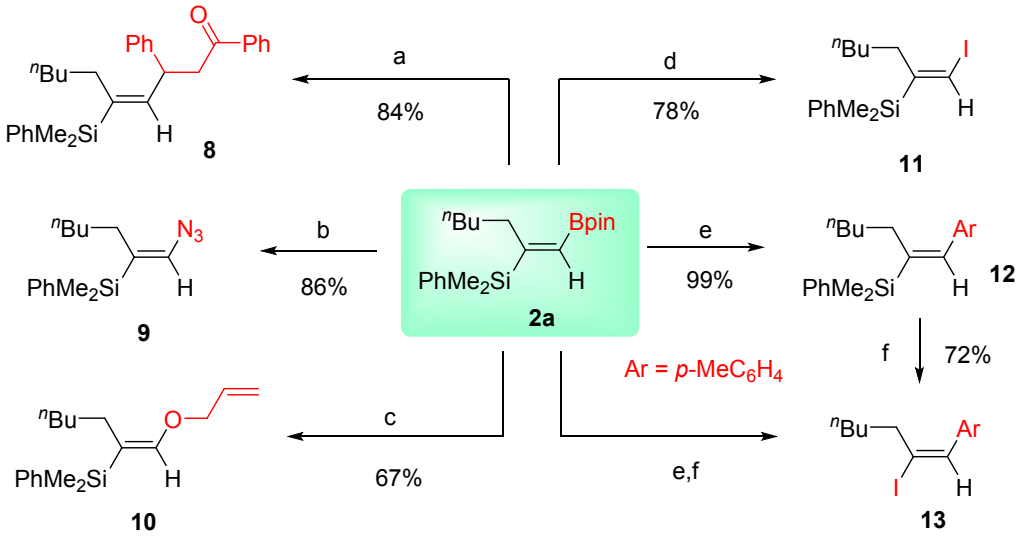

Conditions: (a) (*E*)-chalcone, $[Rh(cod)Cl]_2$, MeOH, H_2O, 90 °C; (b) NaN_3, $CuSO_4$, MeOH, r.t.; (c) allyl alcohol, $Cu(OAc)_2$, Et_3N, r.t.; (d) I_2, NaOH, THF, H_2O, r.t.; (e) 1-*p*-iodotoluene, $PdCl_2(dppf)$, dioxane, KOH, 90 °C; (f) NIS, 2,6-lutidine, $(CF_3)_2CHOH$, 0 °C, 30 min.

Mechanistic Studies

DFT calculations. The above experimental observations raise several mechanistic questions: (1) Why and how does hydroboration proceed in the 1,1-addition fashion? (2) How is the stereochemistry of the final product controled? To address these questions, density functional theory (DFT) calculations have been carried out (with SMD M06/6-31G*+SDD(Ru) method, see the SI for details).[14,15] Also, DFT quasi-classical molecular dynamic (MD) simulations[16-18] on the rate-determining step by the same method were performed.

Oxidative hydrogen migration. Similar to the mechanism for the related Ru(II)-catalyzed *trans*-hydrofunctionalization and *gem*-hydrogenation reactions proposed by us and Fürstner,[3,8-10] our DFT results suggested that the present hydroboration reaction starts by ligand exchange with HBpin and alkyne followed by the rate-determining oxidative hydrogen migration to the alkyne carbon substituted with the silyl group via **B1a-TS** (Figure 1). Such oxidative hydrogen migration, featuring considerable H···B interaction (1.82 Å, Figure 2), requires a barrier of about 23.3 kcal/mol above **CAT** and directly forms the key metallocyclopropene intermediate **B2a**.[19] In comparison, the other two pathways, oxidative boryl migration via **B1c-TS** or oxidative hydrogen migration with opposite regioselectivity via **B1b-TS**, have higher barriers by 1.8–3.5 kcal/mol. In addition, **B1a-TS** is lower in free energy than the two intermediates involved in the classical metal vinylidene pathway[10b] by more

than 4.1 kcal/mol (Figure S12). Notably, the computed B···C_β distance in **B2a** is quite short (2.51 Å, shorter than its van der Waals distance, 3.62 Å).[16a] Also, the metallocyclopropene plane and the Ru–B bond in **B2a** are oriented to be roughly coplanar (Figure 2). These two structural features in **B2a** are crucial for the subsequent boryl migration (*vide infra*).

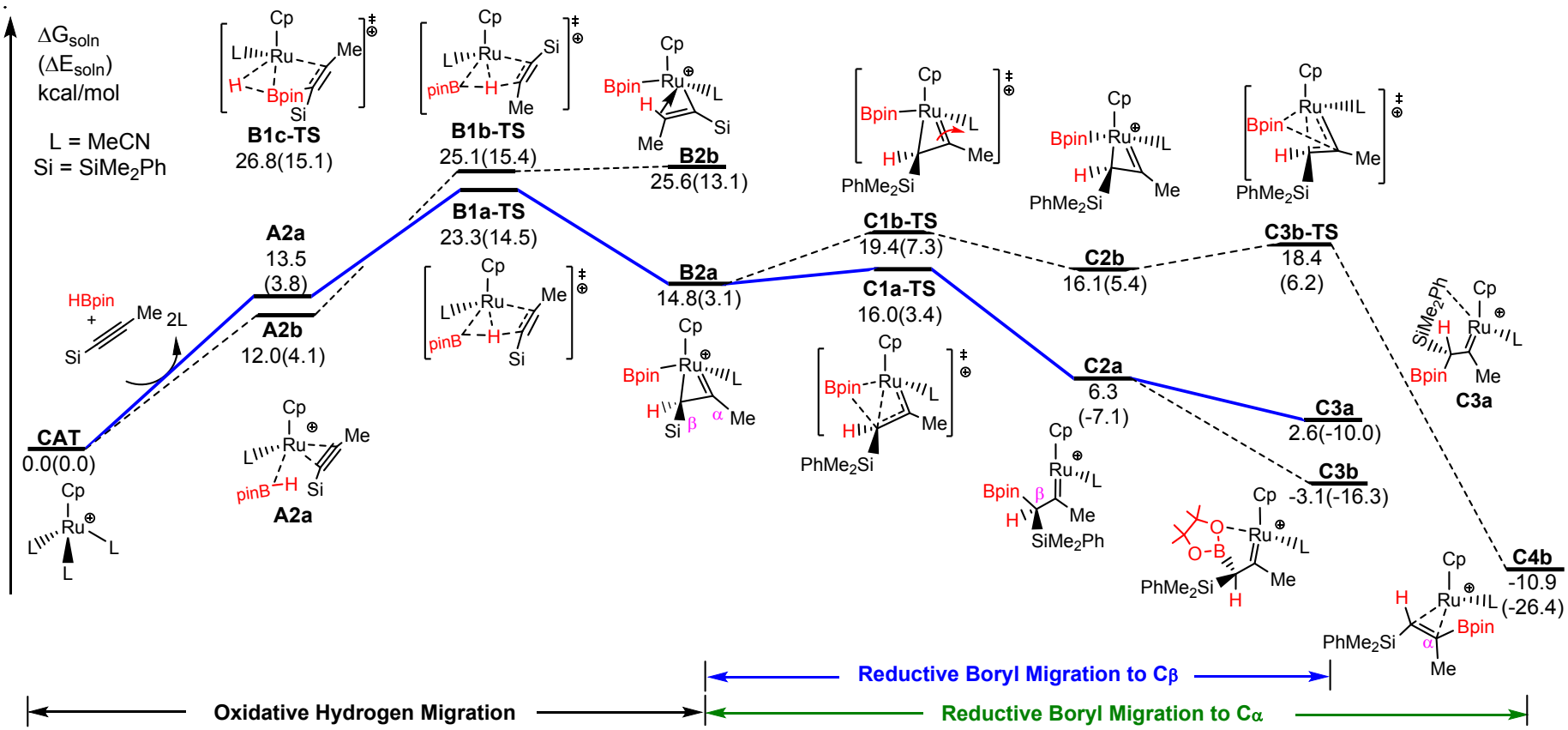

Figure 1. Free energy surface of the most favorable pathway for the initial stage of the *gem*-hydroboration in solution by the SMD M06 method.

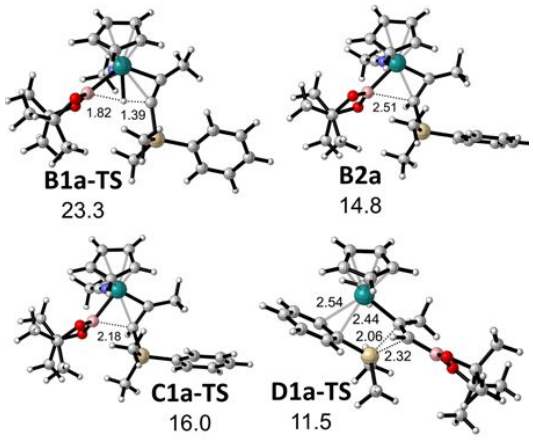

Figure 2. Computed geometries and relative free energies of the key transition states and intermediates for the Ru-catalyzed *gem*-addition of MeC≡CSiPhMe$_2$ by the SMD M06 method.

Next, **B2a** could potentially undergo reductive 1,2-boryl migration to the C_α position and form the regular 1,2-*cis*-hydroboration product **C4b** (Figure 1).[3d] However, this path would require a prior rearrangement to form metallocyclopropene **C2b** (via **C1b-TS**), in which the Ru–B bond becomes roughly perpendicular to the metallocyclopropene plane. Alternatively, a reductive boryl migration to the C_β position in **B2a** via **C1a-TS** to form a new *gem* Ru(II)-carbene intermediate **C2a** preferentially occurs with a lower barrier (~16.0 kcal/mol above **CAT**; only ~1.2 kcal/mol above **B2a**). **C1a-TS** was computed to be lower in free energy than **C1b-TS** by ~3.4 kcal/mol. It is believed that the interaction between the empty p(B) orbital and the filled $\pi(C_\beta{=}C_\alpha)$ orbital in **C1a-TS** as well as their coplanar structural relationship should promote this reductive boryl migration to C_β leading to **C2a**. Although the related reductive hydrogen migration leading to a *gem*-H_2 Ru(II)-carbene intermediate was first discovered by Fürstner and coworkers, such a reductive boryl migration to form a *gem*-(H,B) Ru(II)-carbene is uncommon, which is crucial for the ultimate *gem*-hydroboration product formation (*vide infra*).

Reaction dynamics of oxidative hydrogen migration. Encouraged by the abovementioned very low barrier for the reductive boryl migration via **C1a-TS** (~1.2 kcal/mol above **B2a**) and the recent DFT quasi-classical MD studies on ultrafast dynamics in organic reactions,[16a-c] we envisioned that the initial process from **B1a-TS** to the Ru(II)-carbene intermediate **C2a** might be very fast. Pleasingly, our DFT MD simulations show that roughly 17 trajectories (~24 %) out of the 71 productive trajectories were found to pass by **C1a-TS** and essentially form the C_β–B bond (<1.6 Å) within 1 ps in solution (Figures 3-4 and S3-S9). Also, considerable C_β–B bond formation (<2.18 Å, shorter than that in **C1a-TS**) was observed in ~31% of the trajectories, whereas the C_β···B distance is mainly within 2.8-3.13 Å (~56%, Figure 4). Moreover, the time gap between the C_β–H and C_β–B bond forming processes in these successful trajectories is ~430-965 fs, in which the initial C_β–H bond formation is extremely fast (9-51 fs, see Figures S3-S4). Overall, our DFT MD simulations suggest that an ultrafast formation (~ps) of the *gem*-(H,B) Ru-carbene directly from the initial oxidative hydrogen migration could be possible.

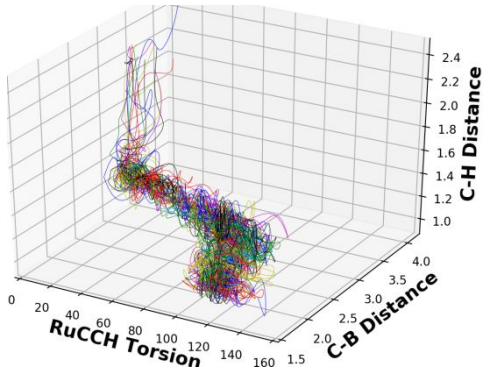

Figure 3. The 17 successful trajectories leading to **B2a** from the rate-determining transition state region (**B1a-TS**) in solution by the SMD M06 method.

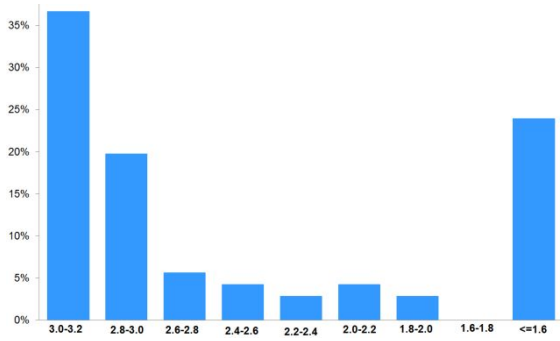

Figure 4. Histogram of the minimum C_β···B distance in all the productive trajectories in solution by the SMD M06 method.

Boryl migration versus silyl migration. After the reductive boryl migration to **C2a**, C–C rotation takes place to give two more stable Ru(II)-carbene isomers **C3a** (with η^2-coordination of the benzene to the metal) and **C3b** (with η^1-coordination of the boryl oxygen atom to the metal, see Figure 5a). Although **C3a** was computed to be less stable than **C3b** by 5.7 kcal/mol, the former has a lower barrier for the 1,2-silyl migration from C_β to C_α via **D1a-TS** than the latter one via **D1b-TS** by 11.3 kcal/mol.[10b] In addition, **D1a-TS** is lower in free energy than **D1a-TS2** (with opposite boryl and hydrogen positions) by 2.2 kcal/mol. **D1a-TS** with the bulky boryl group away from the Cp ring and the silyl group is energetically more favorable and thus leads to the desired and stable (*E*)-type complex **D2a** (Figure 5b). It is worth noting that the silyl migration results in slight bending of the C_α–Ru part (along C_α–C_β bond) away from the incoming silyl group (Figure 5b), which causes Ru to approach C_β from the opposite side (relative to silyl migration). Therefore, this step (**C3a** to **D2a**) can also be viewed as cooperative hopping of the silyl and Ru on the opposite side of the C_β=C_α plane. In contrast, silyl migration via either **D1a-TS2** or **D1b-TS** leading to the less stable (*Z*)-type complex **D2b** is disfavored due to steric repulsion between the boryl and CpRu moieties (Figure 5a). Moreover, the 1,2-silyl

migration overcomes a lower barrier than the related boryl or hydrogen migration by at least 6.5 kcal/mol. Overall, our computational results are in qualitative agreement with the observed exclusive formation of the *gem*-hydroborated (*E*)-olefin products.

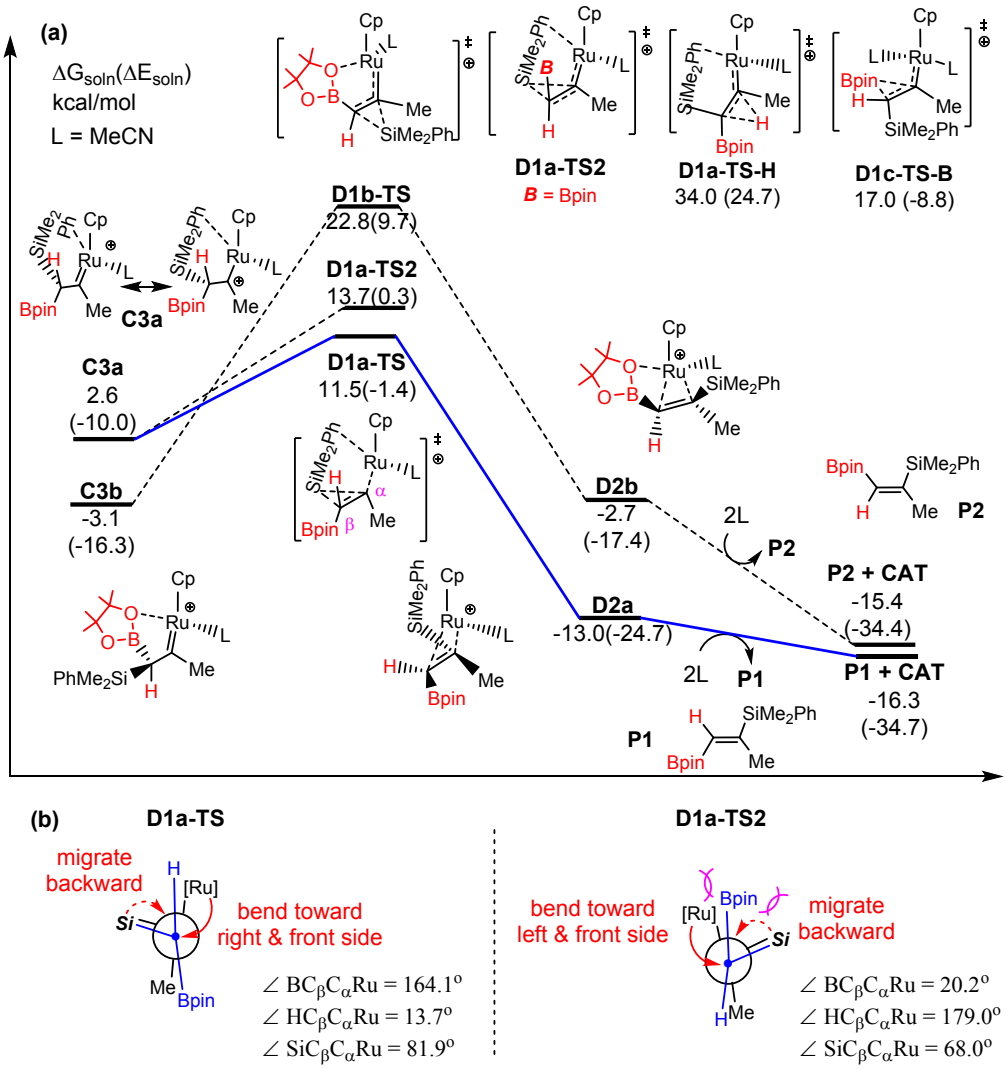

Figure 5. (a) Free energy surface of the most favorable final 1,2-migration pathways in solution by the SMD M06 method. The less favorable pathways for different migrations are given in Figure S10. (b) Newman projection along C_β–C_α in the two key silyl migration transition states with the computed key dihedral angles and relative free energies by the SMD M06 method.

Migration of other groups. To get further insights on the two uncommon migration steps (i.e.

the reductive boryl migration from Ru to C_β in **B2a** and the subsequent silyl migration from C_β to C_α in **C3a**), additional calculations were carried out to probe the migratory propensity of other groups in a similar system (Tables 4 and S7).

As to reductive migration of the X group to C_β (Table 4), our calculations show that the boryl and hydrogen migrations have the lowest migration barriers relative to their preceding metallocyclopropenes (1.2 and 3.2 kcal/mol, respectively). For comparison, the migration of trimethylsilyl (TMS) requires a higher barrier (12.0 kcal/mol). In fact, this barrier is even higher than its alternative migration to C_α leading to 1,2-*trans*-addition according to our previous studies (~5-7 kcal/mol).[3d,9c,10] Moreover, the silyl migration is thermodynamically unfavorable. Furthermore, the migrations of the carbon-based groups, such as -CH_3, -COMe, and -C≡CMe, were also found to have high barriers (10.7-18.6 kcal/mol). Finally, the good π-donating NMe_2 group results in a classical Ru(II) σ-vinyl intermediate with a high migration barrier of 34.8 kcal/mol. Overall, these computational results suggest that the presence of a suitable orbital (e.g. s(H), p(B) or π*(CC)) on the migrating group to interact with the filled π(C_β=C_α) orbital should play a pivotal role in facilitating migration (see Figure S11b).

Table 4. Computed Reductive Migration of X to C_β in the Metallocyclopropene Intermediate[a]

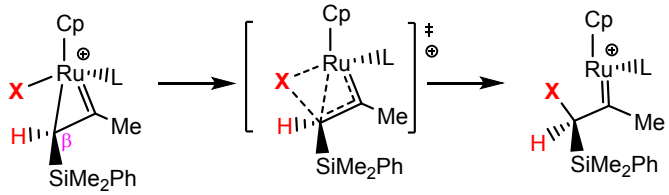

B2a(X) **C1a-TS(X)** **C2a(X)**

X	B2a(X)	C1a-TS(X)	C2a(X)
Bpin	0.0	1.2	-8.5
H	0.0	3.2	-10.0
CH_3	0.0	18.6	-17.6

-C≡CMe	0.0	11.9	-17.8
COMe	0.0	10.7	-21.2
$SiMe_3$	0.0	12.0	0.3
NMe_2[b]	0.0	34.8	-11.9

[a] Computed relative free energies (kcal/mol) in solution by the SMD M06 method. [b] A Ru(II)-vinyl intermediate was formed instead of the metallocyclopropene.

Control Experiments. Although efforts to directly characterize the key *gem*-(H,B) Ru-carbene intermediate or intramolecular trap it were not successful, we carried out some control experiments to further substantiate this mechanism. First of all, it might be possible for silyl alkynes to undergo prior silyl migration to form a metal vinylidene intermediate, which can potentially lead to *gem*-hydroboration. While our DFT calculations suggested this pathway is unfavorable (see Figure S12), we also designed experiments to distinguish between these two paths (Schemes 4 and S1). Silyl alkyne **14**, which bears a propargylic silyl group, was subjected to the standard hydroboration conditions. In addition to the major 1,2-hydroboration product **15a**, two *gem*-hydroboration products **15b** and **15c** were also formed, albeit in low yield (Scheme 4A). In fact, both **15b** and **15c** were likely generated from the common *gem*-(H,B) Ru-carbene **IM2** by the two different silyl migration paths. In contrast, if the reaction proceeds via Ru-vinylidene **IM3**, only product **15c** (but not **15b**) should be expected, which is obviously inconsistent with the experimental results. Furthermore, to favor *gem*-addition (over 1,2-addition) and minimize the perturbation by the migratory ability of different silyl groups, alkyne **16** bearing two same $PhMe_2Si$ groups was prepared and subjected to the standard conditions. Expectedly, *gem*-hydroboration products **17a** and **17b** were both observed (Scheme 4B). Similarly, the presence of both products is more consistent with the intermediacy of carbene **IM4** than vinylidene **IM5**, which would only lead to **17b**. Finally, alkyne **18**, with carbon in place of the silicon atom in **16**, was also examined (Scheme 4C). It should be unlikely to involve a metal vinylidene intermediate

for **18**. While an unidentifiable mixture was observed with $[CpRu(MeCN)_3]PF_6$ as catalyst, the use of $[Cp^*RuCl]_4$ led to product **19**, which is consistent with the involvement of *gem*-(H,B) Ru-carbene **IM6** as well as the high migration barrier calculated for the $PhMe_2C$ group (Table S7).

Scheme 4. Differentiation between Ru-Vinylidene and *gem*-Hydroborated Ru-Carbene Intermediates

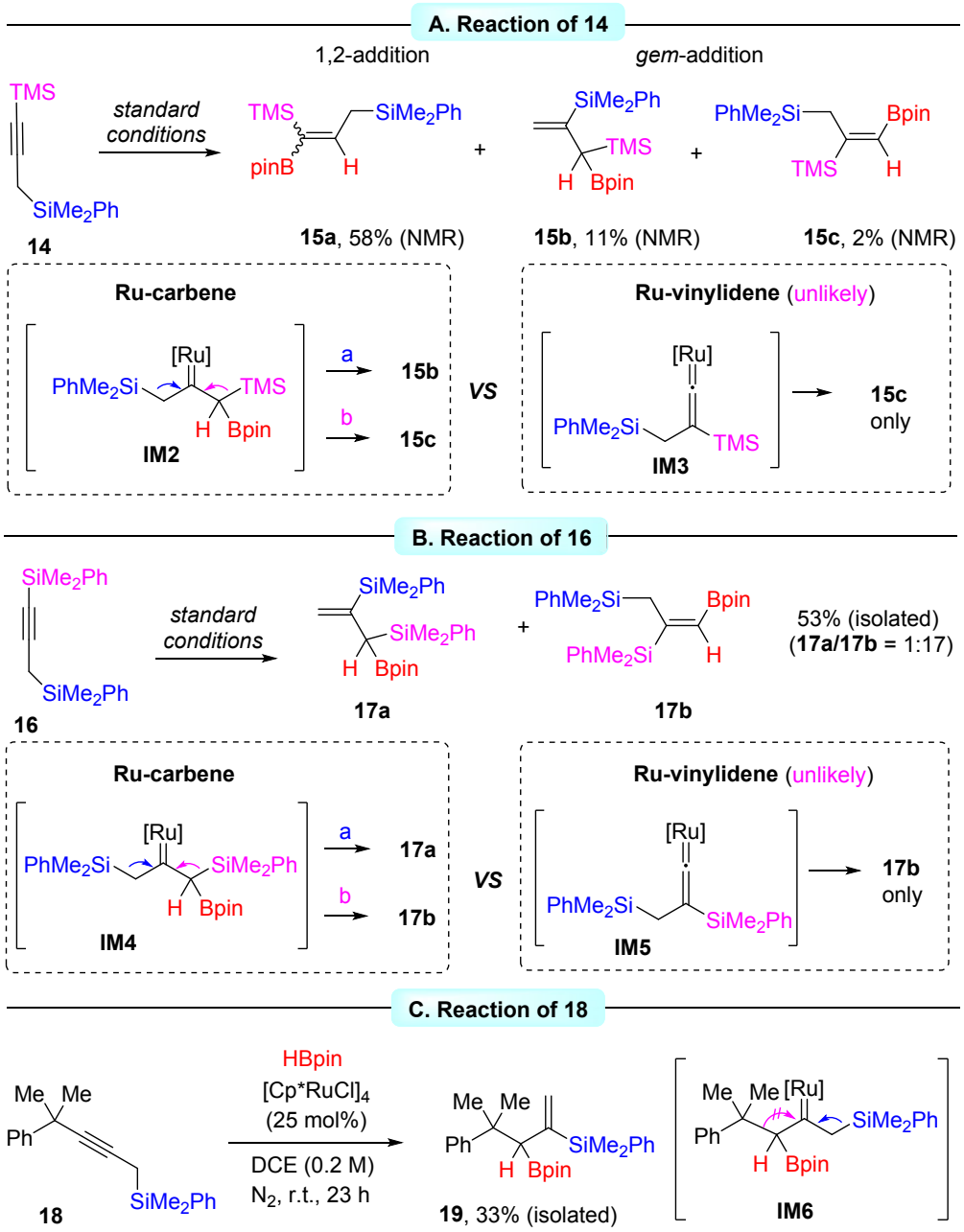

Another possible mechanism for silyl migration might involve dissociation of the substrate to form a silyl cation (due to β-Si effect) followed by re-association (Scheme S1). To distinguish from this possibility, we carried out a cross-over experiment (Scheme 5). The standard hydroboration of a 1:1 mixture of alkynes **1n** and **1s** led to exclusive formation of vinyl boronates **2n** and **2s**. The cross-over products **2n′** and **2s′** were not observed, thereby ruling out the dissociative pathway.

Scheme 5. Cross-over Experiment

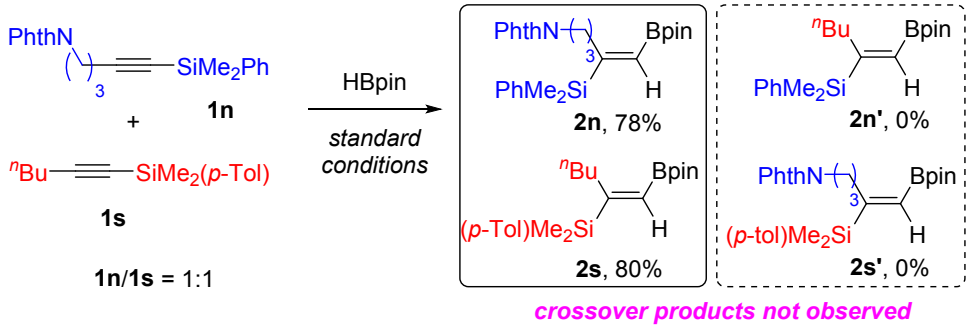

Finally, control experiments were also designed to understand the mechanism of 1,2-hydrosilylation of alkynyl boronate **6** shown in Scheme 2, which led to the same vinyl boronates from *gem*-hydroboration of silyl alkynes. Under the standard conditions, hydrosilylation of alkynyl boronate **20** bearing a propargylic silyl group led to exclusive formation of 1,2-addition product **17b** as a *Z/E* mixture (Scheme 6A). If the *gem*-addition intermediate **IM4** is involved, a mixture of **17a** and **17b** (see Scheme 4B) should be expected. However, the migratory product **17a** was not observed, suggesting that this hydrosilylation may not proceed via *gem*-addition mechanism. In retrospect, we also suspected that our previous discovery on hydrosilylation of silyl alkynes may also possibly proceed via *gem*-addition mechanism.[10a] Therefore, two pairs of

silyl alkynes (**1a** and **22**) with different silanes (Et_3SiH and $PhMe_2SiH$) were employed for cross-check (Scheme 6B). If *gem*-hydrosilylation is operative, the common intermediate **IM7** should be involved and the subsequent silyl migration is expected to give the same products. However, these two reactions proceeded cleanly and selectively to form their own 1,2-*syn*-addition products **21** and **23**, respectively. These results ruled out the *gem*-addition mechanism and further supported the previously established hydrosilylation mechanism, which is also consistent with our calculations shown in Table 4 and highlights the importance of orbital interaction when forming the *gem*-addition Ru-carbene intermediates.[9c,10a]

Scheme 6. Possibility of the Related *gem*-Hydrosilylation

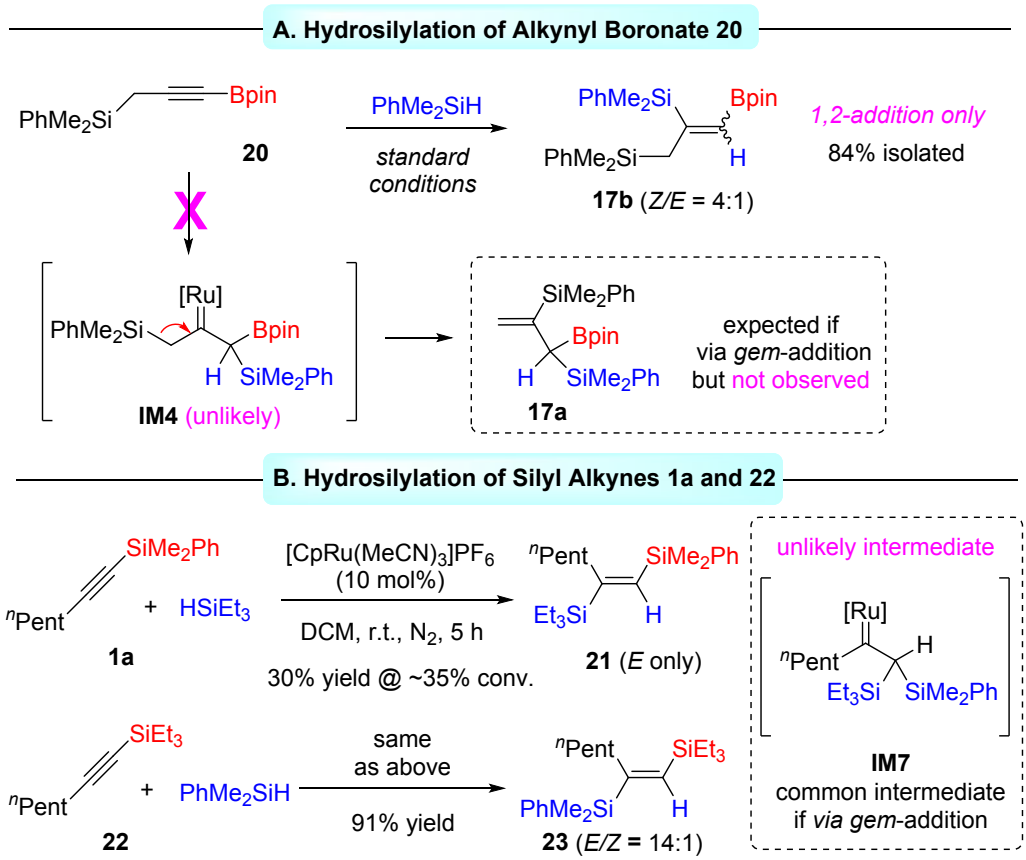

Conclusion

We have developed the a new migratory geminal hydroboration of alkynes. With the proper choice of a [CpRu]-based catalyst, a range of silyl alkynes overcame the intrinsic 1,2-addition propensity observed for general internal alkynes and reacted in a 1,1-addition mode with concomitant silyl migration, providing efficient access to various vinyl boronates with excellent stereoselectivity. These stereodefined boryl- and silyl-substituted olefin products have been demonstrated as useful precursors toward other diversely substituted olefins with defined configuration. The mild reaction conditions can tolerate a wide range of functional groups, including free acid and alcohol, as proved by our scope study and additive compatibility study. This process can also be successfully extended to germanyl alkynes. Mechanistically, unlike the established Ru-catalyzed 1,2-*trans*-hydrometallation, this process features a new pathway involving the key α-boryl-α-silyl Ru-carbene intermediate (Scheme S1). It is noteworthy that this is the first demonstration of such *gem*-addition beyond hydrogenation. DFT (including molecular dynamics) calculations and a series of control experiments provided important insights into mechanistic understanding. The coplanar relationship between the boron atom and the ruthenacyclopropene ring preceding boron migration enables an interaction between the empty *p*(B) orbital and the filled π-type C_α–C_β orbital, which is the key bonding feature responsible for the subsequent unusual reactivity. Control experiments with a range of substrates bearing propargylic silyl group together with the cross-over experiments provided diagnostic information toward the carbene pathway and ruled out the vinylidene and dissociative pathways. Finally, although hydrosilylation of vinyl boronates provided access to the same type products, control experiments indicated that these reactions proceed via normal 1,2-addition pathway, rather than *gem*-addition followed by silyl migration. This study represents a new step forward not only for alkyne hydroboration, but also for more general geminal additions of alkynes.

ASSOCIATED CONTENT

Supporting Information

The Supporting Information is available free of charge via the Internet at http://pubs.acs.org.

Experimental and computational details and NMR data (PDF).

X-ray crystallography data (CIF)

Movie of one successful trajectory (MP4).

AUTHOR INFORMATION

Corresponding Author

*Email to

J. S.: sunjw@ust.hk

Y.-D. W.: wuyd@pkusz.edu.cn

L. W. C.: oscarchung@sustech.edu.cn

Notes

The authors declare no competing financial interest.

Acknowledgment: We gratefully acknowledge the financial support from the Research Grants Council of Hong Kong (GRF 16302719), National Natural Science Foundation of China (21672096, 21873043, 21933003, 21933004, 91956114, 21572192) and Shenzhen Science and Technology Innovation Committee (JCYJ20170412150507046, JCYJ20170817104736009), the Shenzhen Nobel Prize Scientists Laboratory Project (C17783101), and Guangdong Provincial Key Laboratory of Catalysis (2020B121201002). We thank Profs. Guochen Jia and Xinhao

Zhang for helpful discussion and the Center for Computational Science and Engineering at the Southern University of Science and Technology for partial support on this work.

References

(1) (a) Lennox, A. J. J.; Lloyd-Jones, G. C. Selection of Boron Reagents for Suzuki−Miyaura Coupling. *Chem. Soc. Rev.* **2014**, *43*, 412−443. (b) Wang, H.; Zeng, Y.-F.; Lv, W.-X.; Tan, D.-H. Synthetic Transformations of Alkenyl MIDA Boronates toward the Efficient Construction of Organoborons. *Synlett* **2018**, *29*, 1415−1420. (c) Yoshida, H. Borylation of Alkynes under Base/Coinage Metal Catalysis: Some Recent Developments. *ACS Catal.* **2016**, *6*, 1799−1811. (d) Carreras, J.; Caballero, A.; Pérez, P. J. Alkenyl Boronates: Synthesis and Applications. *Chem. - Asian J.* **2019**, *14*, 329−343.

(2) *Syn* addition: (a) Brown, H. C.; Gupta, S. K. Catecholborane (1,3,2-benzodioxaorole) as a New, General Monohydroboration Reagent for Alkynes. Convenient Synthesis of Alkeneboronic Esters and Acids from Alkynes via Hydroboration. *J. Am. Chem. Soc.* **1972**, *94*, 4370−4371. (b) Soderquist, J. A.; Colberg, J. Valle, L. D. The Hydroboration of Silylacetylenes. The "Silyl-Markovnikov" Hydroboration Route to Pure (2)-1-(2-Borylviny1)silanes and β-Keto Silanes. *J. Am. Chem. Soc.* **1989**, *111*, 4873−4878. (c) Tucker, C. E.; Davidson, J.; Knochel, P. Mild and Stereoselective Hydroborations of Functionalized Alkynes and Alkenes Using Pinacolborane. *J. Org. Chem.* **1992**, *57*, 3482–3485. (d) Pereira, S.; Srebnik, M. Hydroboration of Alkynes with Pinacolborane Catalyzed by $HZrCp_2Cl$. *Organometallics* **1995**, *14*, 3127–3128. (e) He, X.; Hartwig, J. F. True Metal-Catalyzed Hydroboration with Titanium. *J. Am. Chem. Soc.* **1996**, *118*, 1696−1702. (f) Jang, H.; Zhugralin, A. R.; Lee, Y.; Hoveyda, A. H. Highly Selective Methods for Synthesis of Internal (α-) Vinylboronates through Efficient NHC–Cu-Catalyzed

Hydroboration of Terminal Alkynes. Utility in Chemical Synthesis and Mechanistic Basis for Selectivity. *J. Am. Chem. Soc.* **2011**, *133*, 7859−7871. (g) Guo, J.; Cheng, B.; Shen, X.; Lu, Z. Cobalt-Catalyzed Asymmetric Sequential Hydroboration/Hydrogenation of Internal Alkynes. *J. Am. Chem. Soc.* **2017**, *139*, 15316−15319.

(3) Pioneering *trans*-hydroboration with cationic Ru-system: (a) Sundararaju, B.; Fürstner, A. A *trans*-Selective Hydroboration of Internal Alkynes. *Angew. Chem., Int. Ed.* **2013**, *52*, 14050−14054. (b) Longobardi, L. E. L.; Fürstner, A.; Longobardi, L. E. L. *trans*-Hydroboration of Propargyl Alcohol Derivatives and Related Substrates. *Chem. Eur. J.* **2019**, *25*, 10063−10068. (c) Fürstner, A. *trans*-Hydrogenation, *gem*-Hydrogenation, and *trans*-Hydrometalation of Alkynes: An Interim Report on an Unorthodox Reactivity Paradigm. *J. Am. Chem. Soc.* **2019**, *141*, 11−24. (d) Song, L.-J.; Wang, T.; Zhang, X.; Chung, L. W.; Wu, Y.-D. A Combined DFT/IM-MS Study on the Reaction Mechanism of Cationic Ru(II)-Catalyzed Hydroboration of Alkynes. *ACS Catal.* **2017**, *7*, 1361−1368.

(4) Other transition-metal-catalyzed *trans*-hydroborations: (a) Wang, Q.; Motika, S. E.; Akhmedov, N. G.; Petersen, J. L.; Shi, X. Synthesis of Cyclic Amine Boranes through Triazole-Gold(I)-Catalyzed Alkyne Hydroboration. *Angew. Chem., Int. Ed.* **2014**, *53*, 5418−5422. (b) Xu, S.; Haeffner, F.; Li, B.; Zakharov, L. N.; Liu, S.-Y. Monobenzofused 1,4-Azaborines: Synthesis, Characterization, and Discovery of a Unique Coordination Mode. *Angew. Chem., Int. Ed.* **2013**, *52*, 14050−14054. (c) Xu, S.; Zhang, Y.; Li, B.; Liu, S.-Y. Site-Selective and Stereoselective *Trans*-Hydroboration of 1,3-Enynes Catalyzed by 1,4-Azaborine-Based Phosphine−Pd Complex. *J. Am. Chem. Soc.* **2016**, *138*, 14566−14569. (d) Jang, W. J.; Lee, W. L.; Moon, J. H.; Lee, J. Y.; Yun, J. Copper-Catalyzed *Trans*-Hydroboration of Terminal Aryl Alkynes: Stereodivergent Synthesis of Alkenylboron Compounds. *Org. Lett.* **2016**, *18*, 1390−1393. (e) Yamamoto, K.; Mohara, Y.; Mutoh, Y.;

Saito S. Ruthenium-Catalyzed (*Z*)-Selective Hydroboration of Terminal Alkynes with Naphthalene-1,8-diaminatoborane. *J. Am. Chem. Soc.* **2019**, *141*, 17042−17047.

(5) Terminal alkyne *gem*-addition via metal vinylidenes: (a) Ohmura, T.; Yamamoto, Y.; Miyaura, N. Rhodium- or Iridium-Catalyzed *trans*-Hydroboration of Terminal Alkynes, Giving (Z)-1-Alkenylboron Compounds. *J. Am. Chem. Soc.* **2000**, *122*, 4990−4991. For a mechanistic study, see: (b) Cid, J.; Carbó, J. J.; Fernández, E. Catalytic Nonconventional *trans*-Hydroboration: A Theoretical and Experimental Perspective. *Chem. Eur. J.* **2012**, *18*, 1512−1521. (c) Gunanathan, C.; Hölscher, M.; Pan, F.; Leitner, W. Ruthenium Catalyzed Hydroboration of Terminal Alkynes to *Z*-Vinylboronates. *J. Am. Chem. Soc.* **2012**, *134*, 14349−14352.

(6) Terminal alkyne *gem*-addition via metal acetylides and alkynyl boronates: (a) Obligacion, J. V.; Neely, J. M.; Yazdani, A. N.; Pappas, I.; Chirik, P. J. Cobalt Catalyzed *Z*-Selective Hydroboration of Terminal Alkynes and Elucidation of the Origin of Selectivity. *J. Am. Chem. Soc.* **2015**, *137*, 5855−5858. (b) Gorgas, N.; Alves, L. G.; Stöger, B.; Martins, A. M.; Veiros, L. F.; Kirchner, K. Stable, Yet Highly Reactive Nonclassical Iron(II) Polyhydride Pincer Complexes: *Z*-Selective Dimerization and Hydroboration of Terminal Alkynes. *J. Am. Chem. Soc.* **2017**, *139*, 8130−8133. For a mechanistic study, see: (c) Gorgas, N.; Stöger, B.; Veiros, L. F.; Kirchner, K. Iron(II) Bis(acetylide) Complexes as Key Intermediates in the Catalytic Hydrofunctionalization of Terminal Alkynes. *ACS Catal.* **2018**, *8*, 7973−7982.

(7) For selected examples using non-transition-metal catalysts: (a) McGough, J. S.; Butler, S. M.; Cade, I. A.; Ingleson, M. J. Highly Selective Catalytic *trans*-Hydroboration of Alkynes Mediated by Borenium Cations and $B(C_6F_5)_3$. *Chem. Sci.* **2016**, *7*, 3384−3389. (b) Shimoi, M.; Watanabe, T.; Maeda, K.; Curran, D. P.; Taniguchi, T. Radical *trans*-Hydroboration of

Alkynes with N-Heterocyclic Carbene Boranes. *Angew. Chem., Int. Ed.* **2018**, *57*, 9485−9490. For an example involving borenium-induced silyl shift in bis(silyl)ethynes: (c) Boussonnière, A.; Pan, X.; Geib, S. J.; Curran, D. P. Borenium-Catalyzed Hydroborations of Silyl-Substituted Alkenes and Alkynes with a Readily Available N-Heterocyclic Carbene−Borane. *Organometallics* **2013**, *32*, 7445−7450.

(8) Examples of *gem*-hydrogenation: (a) Radkowski, K., Sundararaju, B.; Fürstner, A. A Functional-group-tolerant Catalytic *Trans* Hydrogenation of Alkynes. *Angew. Chem., Int. Ed.* **2013**, *52*, 355−360. (b) Fuchs, M.; Fürstner, A. *trans*-Hydrogenation: Application to a Concise and Scalable Synthesis of Brefeldin A. *Angew. Chem., Int. Ed.* **2015**, *54*, 3978−3982. (c) Leutzsch, M.; Wolf, M. L.; Gupta, P.; Fuchs, M.; Thiel, W.; Farès, C.; Fürstner, A. Formation of Ruthenium Carbenes by *gem*-Hydrogen Transfer to Internal Alkynes: Implications for Alkyne *trans*-Hydrogenation. *Angew. Chem., Int. Ed.* **2015**, *54*, 12431−12436. (d) Guthertz, A.; Leutzsch, M.; Wolf, L. M.; Gupta, P.; Rummelt, S. M.; Goddard, R.; Farès, C.; Thiel, W.; Fürstner, A. Half-Sandwich Ruthenium Carbene Complexes Link *trans*-Hydrogenation and *gem*-Hydrogenation of Internal Alkynes. *J. Am. Chem. Soc.* **2018,** *140*, 3156−3169. (e) Biberger, T.; Gordon, C. P. Leutzsch, M.; Peil, S.; Guthertz, A.; Copéret, C.; Fürstner, A. Alkyne *gem*-Hydrogenation: Formation of Pianostool Ruthenium Carbene Complexes and Analysis of Their Chemical Character. *Angew. Chem., Int. Ed.* **2019**, *58*, 8845−8850.

(9) Ru-catalyzed hydrosilylation: (a) Trost, B. M.; Ball, Z. T. Markovnikov Alkyne Hydrosilylation Catalyzed by Ruthenium Complexes. *J. Am. Chem. Soc.* **2001**, *123*, 12726−12727. (b) Trost, B. M.; Ball, Z. T. Intramolecular Endo-Dig Hydrosilylation Catalyzed by Ruthenium: Evidence for a New Mechanistic Pathway. *J. Am. Chem. Soc.* **2003**, *125*, 30−31. (c) Chung, L. W.; Wu, Y.-D.; Trost, B. M.; Ball, Z. T. A Theoretical

Study on the Mechanism, Regiochemistry, and Stereochemistry of Hydrosilylation Catalyzed by Cationic Ruthenium Complexes. *J. Am. Chem. Soc.* **2003**, *125*, 11578−11582. (d) Trost, B. M.; Ball, Z. T. Alkyne Hydrosilylation Catalyzed by a Cationic Ruthenium Complex: Efficient and General *Trans* Addition. *J. Am. Chem. Soc.* **2005**, *127*, 17644−17655. (e) Rummelt, S. M.; Fürstner, A. Ruthenium-Catalyzed *trans*-Selective Hydrostannation of Alkynes. *Angew. Chem., Int. Ed.* **2014**, *53*, 3626−3630. (f) Rummelt, S. M.; Radkowski, K.; Roşca, D.-A.; Fürstner, A. Interligand Interactions Dictate the Regioselectivity of *trans*-Hydrometalations and Related Reactions Catalyzed by [Cp*RuCl]. Hydrogen Bonding to a Chloride Ligand as a Steering Principle in Catalysis. *J. Am. Chem. Soc.* **2015**, *137*, 5506−5519. (g) Roşca, D.-A.; Radkowski, K.; Wolf, L. M.; Wagh, M.; Goddard, R.; Thiel, W.; Fürstner, A. Ruthenium-Catalyzed Alkyne *trans*-Hydrometalation: Mechanistic Insights and Preparative Implications. *J. Am. Chem. Soc.* **2017**, *139*, 2443−2455. (h) Rummelt, S. M.; Cheng, G.-J.; Gupta, P.; Thiel, W.; Fürstner, A. Hydroxy-Directed Ruthenium-Catalyzed Alkene/Alkyne Coupling: Increased Scope, Stereochemical Implications, and Mechanistic Rationale. *Angew. Chem., Int. Ed.* **2017**, *56*, 3599−3604; Corrigendum: **2017**, *56*, 5652.

(10) (a) Ding, S.; Song, L.-J.; Chung, L. W.; Zhang, X.; Sun, J.; Wu, Y.-D. Ligand-Controlled Remarkable Regio- and Stereodivergence in Intermolecular Hydrosilylation of Internal Alkynes: Experimental and Theoretical Studies. *J. Am. Chem. Soc.* **2013**, *135*, 13835−13842. (b) Song, L.; Feng, Q.; Wang, Y.; Ding, S.; Wu, Y.-D.; Zhang, X.; Chung, L. W.; Sun, J. Ru-Catalyzed Migratory Geminal Semihydrogenation of Internal Alkynes to Terminal Olefins. *J. Am. Chem. Soc.* **2019**, *141*, 17441−17451. (c) Song, L.-J.; Ding, S.; Wang, Y.; Zhang, X.; Wu, Y.-D.; Sun, J. Ir-Catalyzed Regio- and Stereoselective Hydrosilylation of Internal Thioalkynes: A Combined Experimental and Computational

Study. *J. Org. Chem.* **2016**, *81*, 6157−6164. (d) Ding, S.; Song, L.-J.; Wang, Y.; Zhang, X.; Chung, L. W.; Wu, Y.-D.; Sun, J. Highly Regio- and Stereoselective Hydrosilylation of Internal Thioalkynes under Mild Conditions. *Angew. Chem., Int. Ed.* **2015**, *54*, 5632−5635.

(11) (a) Anderson, J. C.; Munday, R. H. Vinyldimethylphenylsilanes as Safety Catch Silanols in Fluoride-Free Palladium-Catalyzed Cross-Coupling Reactions. *J. Org. Chem.* **2004**, *69*, 8971−8974. (b) Fleming, I.; Henning, R.; Parker, D. C.; Plaut, H. E.; Sanderson, P. E. J. The Phenyldimethylsilyl Group as a Masked Hydroxy Group. *J. Chem. Soc., Perkin Trans. 1* **1995**, 317−337.

(12) (a) Akiyama, T. Germanium in Organic Synthesis. In *Main Group Metals in Organic Synthesis*; Yamamoto, H., Oshima, K., Eds.; Wiley-VCH Verlag GmbH & Co. KGaA: Weinheim, 2004; pp 593−619. (b) Spivey, A.; Tseng, C.-C. Vinylgermanes. In *Science of Synthesis Knowledge Updates*; Thomas, E. J., Moloney, M. G., Eds.; Thieme: Stuttgart, 2010; Vol. 2010/1, Section 5.1.23.6, pp 49−57.

(13) Collins, K. D.; Glorius, F. A Robustness Screen for the Rapid Assessment of Chemical Reactions. *Nat. Chem.* **2013**, *5*, 597−601.

(14) Mantina, M.; Chamberlin, A. C.; Valero, R.; Cramer, C. J.; Truhlar, D. G. Consistent Van der Waals Radii for the Whole Main Group. *J. Phys. Chem. A* **2009**, *113*, 5806−5812.

(15) (a) Musaev, D. G.; Mebel, A. M.; Morokuma, K. An Ab Initio Molecular Orbital Study of the Mechanism of the Rhodium(I)-catalyzed Olefin Hydroboration Reaction. *J. Am. Chem. Soc.* **1994**, *116*, 10693–10702. (b) Yang, Z. D.; Pal, R.; Hoang, G. L.; Zeng, X. C.; Takacs, J. M. Mechanistic Insights into Carbonyl-directed Rhodium-catalyzed Hydroboration: Ab Initio Study of a Ayclic γ, δ-Unsaturated Amide. *ACS Catal.* **2014**, *4*, 763–773.

(16) (a) Black, K.; Liu, P.; Xu, L.; Doubleday, C.; Houk, K. N. Dynamics, Transition States, and Timing of Bond Formation in Diels-Alder Reactions. *Proc. Natl Acad. Sci. USA* **2012**,

109, 12860−12865. (b) Yang, Z.; Yang, S.; Yu, P.; Li, Y.; Doubleday, C.; Park, J.; Patel, A.; Jeon, B.-s.; Russell, W. K.; Liu, H.-w.; Russell, D. H.; Houk, K. N. Influence of Water and Enzyme SpnF on the Dynamics and Energetics of the Ambimodal [6+4]/[4+2] Cycloaddition. *Proc. Natl Acad. Sci. USA* **2018**, *115*, E848−E855. (c) Jiménez-Osés, G.; Liu, P.; Matute, R. A.; Houk, K. N. Competition Between Concerted and Stepwise Dynamics in the Triplet Di-π-Methane Rearrangement. *Angew. Chem., Int. Ed.* **2014**, *53*, 8664−8667. (d) Kurouchi, H.; Singleton, D. A. Labelling and Determination of the Energy in Reactive Intermediates in Solution Enabled by Energy-dependent Reaction Selectivity. *Nat. Chem.* **2018**, *10*, 237−241. (e) Bailey, J. O.; Singleton, D. A. Failure and Redemption of Statistical and Nonstatistical Rate Theories in the Hydroboration of Alkenes. *J. Am. Chem. Soc*. **2017**, *139*, 15710−15723.

(17) (a) Hong, Y. J.; Tantillo, D. J. Biosynthetic Consequences of Multiple Sequential Post-transition-state Bifurcations. *Nat. Chem.* **2014**, *6*, 104−111. (b) Hare, S. R.; Tantillo, D. J. Cryptic Post-transition State Bifurcations that Reduce the Efficiency of Lactone-forming Rh Carbenoid C-H Insertions. *Chem. Sci*. **2017**, *8*, 1442−1449. (c) Blümel, M.; Nagasawa, S.; Blackford, K.; Hare, S. R.; Tantillo, D. J.; Sarpong, R. Rearrangement of Hydroxylated Pinene Derivatives to Fenchone-Type Frameworks: Computational Evidence for Dynamically-Controlled Selectivity. *J. Am. Chem. Soc.* **2018**, *140*, 9291−9298.

(18) (a) Pratihar, S.; Ma, X.; Homayoon, Z.; Barnes, G. L.; Hase, W. L. Direct Chemical Dynamics Simulations. *J. Am. Chem. Soc*. **2017**, *139*, 3570−3590. (b) Carlsen, R.; Wohlgemuth, N.; Carlson, L.; Ess, D. H. Dynamical Mechanism May Avoid High-Oxidation State Ir(V)-H Intermediate and Coordination Complex in Alkane and Arene C-H Activation by Cationic Ir(III) Phosphine. *J. Am. Chem. Soc*. **2018**, *140*, 11039−11045. (c) Yang, Y.; Zhang, X.; Zhong, L.-P.; Lan, J.; Li, X.; Li, C.-C.; Chung, L. W. Unusual KIE

and Dynamics Effects in the Fe-catalyzed Hetero-Diels-Alder Reaction of Unactivated Aldehydes and Dienes. *Nat. Commun.* **2020**, *11*, 1850.

(19) For precedence of Ru(IV) piano stool complexes with similar coordination environment: (a) Fasulo, M. E.; Glaser, P. B.; Tilley, T. D. Cp*(P^iPr_3)RuOTf: A Reagent for Access to Ruthenium Silylene Complexes. *Organometallics* **2011**, *30*, 5524−5531. (b) Jia, G.; Morris, R. H. Wide Range of pK_a Values of Coordinated Dihydrogen. Synthesis and Properties of Some η^2-Dihydrogen and Dihydride Complexes of Ruthenium. *J. Am. Chem. Soc.* **1991**, *113*, 875−883.

TOC Graphic

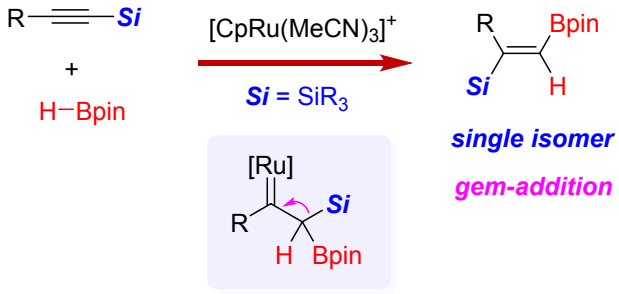
R
Si
+
H–Bpin
[CpRu(MeCN)3]+
Si = SiR3
[Ru]
R
Si
H
Bpin
R
Bpin
Si
H
single isomer
gem-addition